Nuclear Instruments and Methods in Physics Research A 658 (2011) 11–16

Contents lists available at ScienceDirect

Nuclear Instruments and Methods in Physics Research A

journal homepage: www.elsevier.com/locate/nima

Silicon detectors for the sLHC

A. Affolder [a], A. Aleev [b], P.P. Allport [a], L. Andricek [c], M. Artuso [d], J.P. Balbuena [e], L. Barabash [f], T. Barber [g], A. Barcz [h,i], D. Bassignana [e], R. Bates [j], M. Battaglia [k], M. Beimforde [c], J. Bernardini [l], C. Betancourt [k], G.M. Bilei [m], D. Bisello [n], A. Blue [j], J. Bohm [o], G. Bolla [p], A. Borgia [d], L. Borrello [l], D. Bortoletto [p], M. Boscardin [q], M.J. Bosma [r], T.J.V. Bowcock [a], M. Breindl [g], J. Broz [s], M. Bruzzi [t], A. Brzozowski [u], P. Buhmann [v], C. Buttar [j], F. Campabadal [e], A. Candelori [n], G. Casse [a], S. Charron [w], D. Chren [x], S. Cihangir [y], V. Cindro [z], P. Collins [aa], E. Cortina Gil [ab], C.A. Costinoaia [ac], D. Creanza [ad], C. Cristobal [ae], G.-F. Dalla Betta [q], W. de Boer [af], M. De Palma [ad], R. Demina [ag], A. Dierlamm [af], S. Díez [e], D. Dobos [aa], F. Doherty [j], I. Dolenc Kittelmann [aa], Z. Dolezal [s], A. Dolgolenko [f], C. Dragoi [ac], A. Driewer [g], S. Dutta [l], D. Eckstein [v], L. Eklund [j], I. Eremin [ah], V. Eremin [ah], J. Erfle [v], N. Fadeeva [ah], M. Fahrer [aa], F. Fiori [l], C. Fleta [e], E. Focardi [t], D. Forshaw [a], E. Fretwurst [v], M. Frey [af], A.G. Bates [j], C. Gallrapp [aa], C. Garcia [ai], E. Gaubas [aj], M.-H. Genest [w], K. Giolo [p], M. Glaser [aa], C. Goessling [ak], A. Golubev [b], I. Gorelov [al], G. Grégoire [ab], P. Gregori [q], E. Grigoriev [b], A.A. Grillo [k], S. Grinstein [ae], A. Groza [f], J. Guskov [am], T.E. Hansen [an], J. Härkönen [ao], F.G. Hartjes [r], F. Hartmann [af], M. Hoeferkamp [al], R. Horisberger [ap], A. Houdayer [w], D. Hynds [j], I. Ilyashenko [ah], A. Junkes [v], A. Kadys [aj], P. Kaminski [u], A. Karpenko [f], K. Kaska [aa], N. Kazuchits [aq], V. Kazukauskas [aj], A. Kharchuk [b], V. Khivrich [f], J. Kierstead [ar], R. Klanner [v], R. Klingenberg [ak], P. Kodys [s], E. Koffeman [r], M. Köhler [g], Z. Kohout [x], S. Korjenevski [ag], I. Korolkov [ae], R. Kozlowski [u], M. Kozubal [u], G. Kramberger [z], S. Kühn [g], S. Kuleshov [b], A. Kuznetsov [as], S. Kwan [y], A. La Rosa [aa], C. Lacasta [ai], J. Lange [v], K. Lassila-Perini [ao], V. Lastovetsky [f], I. Lazanu [at], S. Lazanu [ac], C. Lebel [w], G. Lefeuvre [d], V. Lemaitre [ab], C. Leroy [w], Z. Li [ar], G. Lindström [v], A. Litovchenko [n], P. Litovchenko [f], M. Lozano [e], Z. Luczynski [u], P. Luukka [ao], A. Macchiolo [c], A. Macraighne [j], T. Mäenpää [ao], L.F. Makarenko [aq], I. Mandic [z], D. Maneuski [j], N. Manna [ad], R. Marco [ai], S. Marti i Garcia [ai], S. Marunko [am], P. Masek [x], K. Mathieson [j], M. Matysek [v], J. Mekki [aa], A. Messineo [l], J. Metcalfe [al], M. Mikestikova [o], M. Mikuž [z], O. Militaru [ab], M. Minano [ai], J. Miyamoto [p], M. Moll [aa], E. Monokhov [as], R. Mori [t], H.-G. Moser [c], D. Muenstermann [ak], F.J. Munoz Sanchez [au], A. Naletko [ah], R. Nisius [c], V. OShea [j], N. Pacifico [aa], D. Pantano [n], C. Parkes [j], U. Parzefall [g,*], D. Passeri [m], M. Pawlowski [u], G. Pellegrini [e], H. Pernegger [aa], M. Petasecca [m], C. Piemonte [q], G.U. Pignatel [m], I. Pintilie [ac], L. Pintilie [ac], K. Piotrzkowski [ab], R. Placekett [j], Th. Pöhlsen [v], L. Polivtsev [f], J. Popule [o], S. Pospisil [x], J. Preiss [g], V. Radicci [ap], R. Radu [ac], J.M. Raf [e], R. Rando [n], R. Richter [c], R. Roeder [av], R. Roger [ae], S. Rogozhkin [b], T. Rohe [ap], S. Ronchin [q], C. Rott [p], A. Roy [p], A. Rummler [ak], A. Ruzin [am], H.F.W. Sadrozinski [k], S. Sakalauskas [aj], N. Samadashvili [aw], M. Scaringella [t], B. Schumm [k], S. Seidel [al], A. Seiden [k], I. Shipsey [p], J. Sibille [ap], P. Sicho [o], T. Slavicek [x], M. Solar [x], U. Soldevila-Serrano [ai], S. Son [p], V. Sopko [x], B. Sopko [x], N. Spencer [k], L. Spiegel [y], A. Srivastava [v], G. Steinbrueck [v], G. Stewart [j], D. Stolze [av], J. Storasta [aj], B. Surma [u], B.G. Svensson [as], P. Tan [y], M. Tomasek [o], K. Toms [al], S. Tsiskaridze [ae], A. Tsvetkov [s], Yu. Tuboltsev [ah], E. Tuominen [ao], E. Tuovinen [ao], T. Tuuva [aw], M. Tylchin [am], H. Uebersee [av], M. Ullán [e], J.V. Vaitkus [aj], M. van Beuzekom [r], E. Verbitskaya [ah], I. Vila Alvarez [au], J. Visser [r], J. Vossebeld [a], V. Vrba [o], M. Walz [g], P. Weigell [c], L. Wiik [g], I. Wilhelm [s], R. Wunstorf [ak], A. Zaluzhny [b], M. Zavrtanik [z], J. Zelazko [u], M. Zen [q], V. Zhukov [af], D. Zontar [z], N. Zorzi [q]

[a] Department of Physics, University of Liverpool, United Kingdom
[b] State Scientific Center of Russian Federation, Institute for Theoretical and Experimental Physics, Moscow, Russia
[c] Max-Planck-Institut fuer Physik, Munich, Germany
[d] Experimental Particle Physics Group, Syracuse University, Syracuse, USA
[e] Centro Nacional de Microelectrónica (IMB-CNM, CSIC), Barcelona, Spain
[f] Institute for Nuclear Research of the Academy of Sciences of Ukraine, Radiation Physics Department, Ukraine
[g] Physikalisches Institut, Albert-Ludwigs Universität Freiburg, D-79104 Freiburg i. Br., Germany

0168-9002/$ - see front matter
doi:10.1016/j.nima.2011.04.045

[h] Institute of Electronics Technology, Warsaw, Poland
[i] Institute of Physics PAS, Warsaw, Poland
[j] Department of Physics & Astronomy, Glasgow University, Glasgow, UK
[k] Santa Cruz Institute for Particle Physics, United States
[l] Universita' di Pisa and INFN sez. di Pisa, Italy
[m] I.N.F.N. and Universit di Perugia, Italy
[n] Dipartimento di Fisica and INFN Sezione di Padova, Via Marzolo 8, I-35131 Padova, Italy
[o] Institute of Physics, Academy of Sciences of the Czech Republic, Praha, Czech Republic
[p] Purdue University, USA
[q] Fondazione Bruno Kessler - FBK, Povo, Trento, Italy
[r] National Institute for Subatomic Physics (Nikhef), Amsterdam, The Netherlands
[s] Charles University Prague, Czech Republic
[t] INFN Florence, Department of Energetics, University of Florence, Italy
[u] Institute of Electronic Materials Technology, Warszawa, Poland
[v] Institute for Experimental Physics, University of Hamburg, Germany
[w] Groupe de la Physique des Particules, Université de Montreal, Canada
[x] Czech Technical University in Prague, Czech Republic
[y] Fermilab, USA
[z] Jožef Stefan Institute and Department of Physics, University of Ljubljana, Ljubljana, Slovenia
[aa] CERN, Geneva, Switzerland
[ab] Université catholique de Louvain, Institut de Physique Nucléaire, Louvain-la-Neuve, Belgium
[ac] National Institute for Materials Physics, Bucharest-Magurele, Romania
[ad] Dipartimento Interateneo di Fisica & INFN, Bari, Italy
[ae] Institut de Física dAltes Energies (IFAE), Bellaterra (Barcelona), Spain
[af] University of Karlsruhe, Institut für Experimentelle Kernphysik, Karlsruhe, Germany
[ag] University of Rochester, United States
[ah] Ioffe Physical-Technical Institute of Russian Academy of Sciences, St. Petersburg, Russia
[ai] IFIC, Joint Research Institute of CSIC and Universitat de Valencia-Estudi General, Valencia, Spain
[aj] Institute of Materials Science and Applied Research, Vilnius University, Vilnius, Lithuania
[ak] Technische Universitaet Dortmund, Lehrstuhl Experimentelle Physik IV, Dortmund, Germany
[al] Department of Physics and Astronomy, University of New Mexico, Albuquerque, NM, USA
[am] Tel Aviv University, Israel
[an] SINTEF ICT, P.O. Box 124, Blindern, N-0314 Oslo, Norway
[ao] Helsinki Institute of Physics, Helsinki, Finland
[ap] Paul Scherrer Institut, Laboratory for Particle Physics, Villigen, Switzerland
[aq] Belarusian State University, Minsk, Belarus
[ar] Brookhaven National Laboratory, Upton, NY, USA
[as] University of Oslo, Physics Department/Physical Electronics, Oslo, Norway
[at] University of Bucharest, Faculty of Physics, Romania
[au] Instituto de Fisica de Cantabria, Spain
[av] CiS Forschungsinstitut für Mikrosensorik und Photovoltaik GmbH, Erfurt, Germany
[aw] Lappeenranta University of Technology, Department of Electrical Engineering, Lappeenranta, Finland

ARTICLE INFO

Available online 7 May 2011

Keywords:
Silicon particle detectors
Radiation damage
Irradiation
Charge collection efficiency

ABSTRACT

In current particle physics experiments, silicon strip detectors are widely used as part of the inner tracking layers. A foreseeable large-scale application for such detectors consists of the luminosity upgrade of the Large Hadron Collider (LHC), the super-LHC or sLHC, where silicon detectors with extreme radiation hardness are required. The mission statement of the CERN RD50 Collaboration is the development of radiation-hard semiconductor devices for very high luminosity colliders. As a consequence, the aim of the R&D programme presented in this article is to develop silicon particle detectors able to operate at sLHC conditions. Research has progressed in different areas, such as defect characterisation, defect engineering and full detector systems. Recent results from these areas will be presented. This includes in particular an improved understanding of the macroscopic changes of the effective doping concentration based on identification of the individual microscopic defects, results from irradiation with a mix of different particle types as expected for the sLHC, and the observation of charge multiplication effects in heavily irradiated detectors at very high bias voltages.

1. Introduction

The upgrade of the LHC to sLHC envisaged for 2020 requires silicon detectors of unprecedented radiation tolerance for the central tracking detectors. Current radiation field simulations for the general-purpose experiments ATLAS [1] and CMS [2] foresee radiation levels of around 2.0×10^{16} n_{eq}/cm^2 for the innermost pixel layers and 1.0×10^{15} n_{eq}/cm^2 for the innermost strip layers.[1] These sLHC fluences exceed the LHC values by about an order of magnitude, and mean that with the sLHC, detectors must enter a new era of radiation hardness, requiring the development of a new generation of silicon detectors.

RD50 is an international collaboration of over 250 scientists from 47 institutes, working on semiconductor detectors to meet the challenges from high luminosity colliders and hence high radiation

* Corresponding author. Tel.: +49 761 203 5756; fax: +49 761 203 5931.
E-mail address: Ulrich.Parzefall@physik.uni-freiburg.de (U. Parzefall).

[1] Non-ionising radiation doses of different particle types and energies are normalised to the silicon crystal lattice damage from neutrons of 1 MeV energy. The unit is 1 MeV neutron-equivalent per cm^2 or in brief n_{eq}/cm^2 [5].

environments [3]. The RD50 activities are grouped into five different research lines: defect and material characterisation, defect engineering, new structures, pad detector characterisation and full detector systems. A full overview of the RD50 activities and results can be found in Ref. [4]. This paper largely concentrates on a number of recent results from a few areas. Amongst those are results from defect characterisation which allow a deeper understanding of the changes of the effective doping concentration N_{eff} as a function of radiation dose, as well as results from 3D detectors which form an essential part of the new structures research line.

2. Radiation damage

In order to understand the technological challenges posed by sLHC radiation levels, it is first necessary to briefly discuss the key radiation effects that adversely affect the sensors. There are three such effects on the sensor bulk material. The first one is an increase of the reverse current (leakage current) in the sensor. The radiation-induced extra current is proportional to the particle fluence when normalised to the damage of neutrons with 1 MeV energy according to the Non-Ionising Energy Loss (NIEL) model. See Ref. [5] and references given therein for more details.

The second effect is the change of the effective doping concentration of the sensor, which in general proceeds through the processes of donor removal and acceptor generation and for a long time has been thought to manifest itself as the device becoming more and more p-type. In consequence, a p-type sensor would stay p-type with an ever increasing N_{eff}, and an n-type sensor would in addition undergo an initial type inversion from n to p. Recent results, some of which are presented in this paper, indicate that not all silicon materials behave in this way. In addition, results from detectors that were irradiated in two steps with protons and neutrons indicate that again for some silicon materials, there may be cancellation effects for the two particle types, rather than the simple accumulation of radiation damage as expected from traditional models.

The third effect is the introduction of defects that can trap drifting signal charges in the silicon bulk. Such defects act as trapping centres, effectively reducing the charge collection efficiency (CCE) of the sensor.

3. Doping concentration

The basic macroscopic radiation effects on the effective doping concentration as described in Section 2 have already been observed by RD48 [6,7], the predecessor of the RD50 Collaboration. Recent studies [8] indicate that these effects for oxygen-enriched n-type epitaxial silicon have a strong dependence on the particle type, exhibiting a significant difference between the results from proton and neutron irradiations and hence violating the simple NIEL scaling hypothesis. Thermally Stimulated Current (TSC) measurements were used to identify the microscopic defects in terms of their activation energy and defect concentration.

Fig. 1 shows key results from the TSC measurements [9,10] for two epitaxial silicon samples with 72 μm thickness irradiated to the equivalent fluence of 1.0×10^{14} n_{eq}/cm^2. One sample was irradiated with 23 GeV protons from the CERN-PS, whereas the other irradiation was performed with reactor neutrons from the TRIGA reactor in Ljubljana. It is evident in the TSC spectra that the proton irradiation produces a much higher concentration of the $E(30\,K)$ defect compared to the neutron irradiation. For the other defects, the differences between the two particle types used for irradiation are much less significant. $E(30\,K)$ is a defect that has a donor level in the upper part of the band gap, and its creation is visible as donor generation leading to a positive space charge (SC) in the silicon bulk.

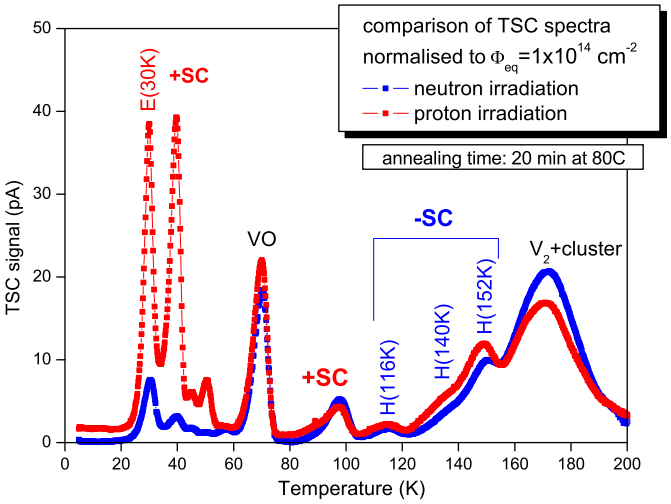

Fig. 1. TSC spectra measured on n-type epitaxial silicon diodes after proton or neutron irradiation to an equivalent fluence of 1.0×10^{14} n_{eq}/cm^2 and 20 min of annealing at 80 °C.

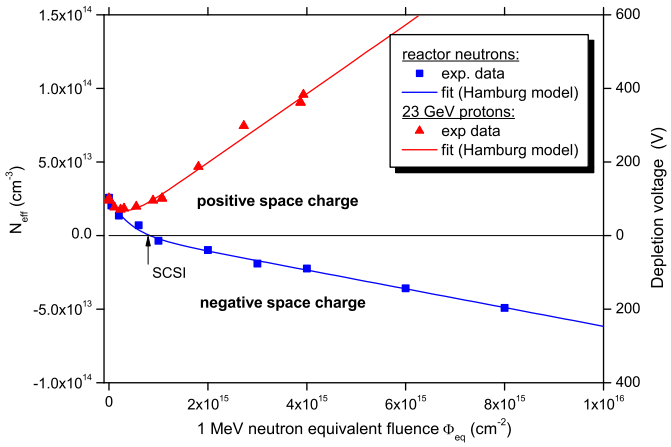

Fig. 2. Effective doping concentration N_{eff} as measured in n-type EPI-diodes as a function of equivalent fluence for both reactor neutron and CERN PS proton irradiations.

Measurements like the one shown in Fig. 1 where performed on a large number of samples irradiated to a set of fluences from a few 10^{14} n_{eq}/cm^2 ranging up to 5.0×10^{15} n_{eq}/cm^2. Again, both neutron and proton irradiations were used. For the same samples, a macroscopic measurement of the Capacitance–Voltage (C–V) characteristics was conducted. The C–V measurements, summarised in Fig. 2, allow extraction of the effective doping concentration in each sample. The N_{eff} plot shows a striking difference between the effects of the two irradiation types observed in the epitaxial silicon material. Proton irradiation will increase the concentration of donors present in the detector, without the silicon undergoing Space Charge Sign Inversion (SCSI). Irradiation with reactor neutrons will lead to SCSI before 10^{15} n_{eq}/cm^2, with the silicon becoming more and more dominated by acceptor-like states which with the help of Fig. 1 can be traced to the H-group of defects from 116 to 152 K. These dominate the space charge in the absence of the $E(30\,K)$ defect.

4. Mixed irradiations

The radiation field inside sLHC experiments will, as in the LHC, be composed mainly from pions, protons and neutrons. The relative

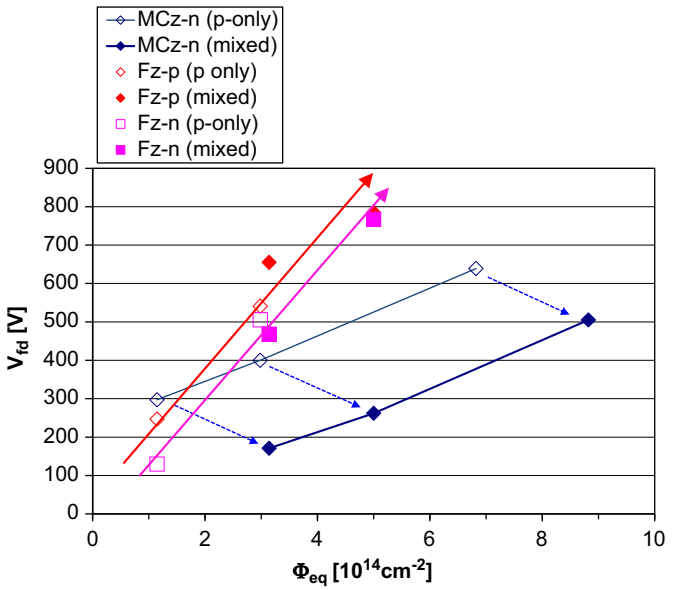

Fig. 3. Full depletion voltage measurements for irradiated silicon pad detector samples as a function of equivalent radiation dose. Results for FZ-p, FZ-n and MCz-n detectors are shown. The arrows (drawn in the same colour code as the samples) indicate the direction of change from the proton-irradiated samples (unfilled symbols) to the ones subjected to mixed irradiations (filled symbols). (For interpretation of the references to color in this figure legend, the reader is referred to the web version of this article.)

composition of the total fluence has a complex dependency on e.g. the radial distance to the interaction point, but generally speaking the radiation levels drop steeply as the radius increases, and pions dominate the short radii up to around 15 cm whereas neutrons tend to dominate from 30 cm outward. A number of studies such as the one reported in Section 3 have shown that irradiations with charged or neutral particles of the same equivalent fluence may have different results in terms of the effective doping concentration and hence the easier accessible full depletion voltage. A key question in this context is to what extent the results from irradiations to an equivalent fluence with a single particle type can be extrapolated to the mixed radiation field of the sLHC.

A dedicated study was performed in the framework of RD50, where a large number of pad detectors of p- and n-type silicon were irradiated first with charged hadrons and then with neutrons [11]. In general, the damage produced by both irradiations was found to add up, for example for the increase of leakage current and trapping. However, in case of the effective doping concentration, a strong material dependency was found. Fig. 3 shows the results of full depletion voltage (V_{fd}) measurements on Float-Zone (FZ) and Magnetic Czochralski (MCz) silicon pad diodes that were exposed to either proton-only or subsequent proton and neutron irradiations. The samples were irradiated to a number of accumulated equivalent fluences up to 9.0×10^{14} n_{eq}/cm^2.

The results indicate that for the FZ silicon material, the radiation effects of both particle types accumulate. For the MCz it appears that the proton irradiation was partially compensated by the following neutron irradiation. A likely explanation for this are stable donors that were introduced in the MCz-n detectors by charged hadron irradiation and were later compensated by introduction of acceptors from the neutron irradiation. As a result the full depletion voltage decreased with increasing neutron fluence.

5. Charge collection

The radiation damage effects mentioned in Section 2 mean a number of negative consequences for any silicon detector exposed to radiation fields as they typically appear at hadron collider experiments. The increasing doping concentration manifests itself as an increasing full depletion voltage of the sensor, which may at a certain fluence exceed either the voltage tolerance of the detector or the maximal voltage rating of the HV power supply. The radiation-induced trapping of signal carriers results in a reduction of the signal measured with the sensor, and hence reduces the signal-to-noise ratio of the detector. This effect can still be worsened by growing noise originating from extra shot noise from the additional leakage current generated by deep traps or defects from radiation damage. For the high fluences expected at the inner layers of sLHC experiments, the combination of charge trapping and N_{eff} effects constitutes a serious challenge that can only be met by reading out from the n-side of the detector. This has two advantages. One is that the detector will collect electrons, which are much less affected by trapping due to their high mobility compared to holes. The other advantage is that n-side readout will also work in partially depleted detectors, as the p–n-junction will be formed around the contact between the n-electrodes and the p-bulk. Note that a n-bulk sensor will be transformed to effective p-bulk by radiation. For reasons of cost and simplicity of production, n-in-p detectors turn out to be the most practical choice. Planar silicon n-in-p detectors have been shown to give acceptable CCE still up to fluences in the order of several 10^{15} n_{eq}/cm^2 for reasonable bias voltages, however, the need for high voltage operation becomes more prominent, with fluences of 10^{16} n_{eq}/cm^2 or more requiring biases in excess of 1 kV [12,13].

A radiation-hard technological alternative to traditional planar detectors is the 3D-detector design. This design [14], where electrodes extend into the silicon bulk perpendicular to the detector surface, gains resistance to radiation effects by decoupling the depletion voltage and collection distance from the detector thickness. This means that considerably lower full depletion voltages are required, and the distance that signal charges have to drift before reaching the electrode is significantly reduced, which makes it less likely for the drifting charges to get trapped. 3D p-type silicon strip detectors made in a simplified double-sided 3D design [15,16] were irradiated with 25 MeV protons at the Karlsruhe Compact Cyclotron, equipped with readout electronics from the CMS tracker and placed in a beam of 225 GeV pions at the CERN SPS H2 beamline. Precision tracking was made using the CMS Silicon Beam Telescope (SiBT) [17] provided by the CMS Helsinki group. In this beam test [18], the 3D detectors were run at different bias voltages, and the signal spectra in the detectors were measured using a clustering algorithm. A signal value was extracted from the signal spectra by fitting a convolution of a Landau function and a Gaussian.

Results for the 3D detectors in this test are shown in Fig. 4. Signals in three different 3D detectors were measured as a function of the reverse bias voltage. The signal in the unirradiated detector reaches a plateau at around 50 V and is used to set the scale for full CCE. As expected, both irradiated detectors show lower signal than the unirradiated one at lower bias voltages. However, the signal keeps on rising with increasing bias voltage. For voltages of 200 V and higher, the signal in the irradiated sensors clearly exceeds the one in the unirradiated reference detector. At the largest bias voltage, the measured signal in each of the irradiated sensors corresponds to roughly twice the signal for full CCE. The effect of more charge being measured than the amount of charge originally created by the passing pion can be attributed to charge multiplication occurring due to impact ionisation. Drifting charges accelerated presumably in the very high electric field of the columnar electrode can gain enough energy to create additional electron–hole pairs. This effect has already been observed in p-side readout 3D detectors irradiated with protons at similar fluences [19]. In the n-side readout devices considered here, it is more pronounced because electrons

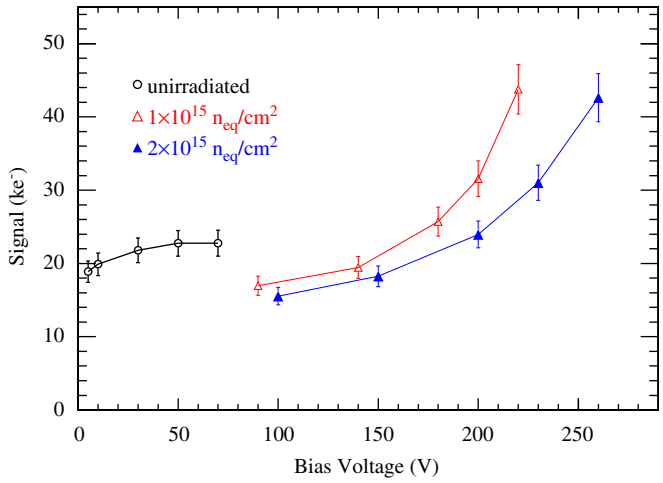

Fig. 4. Signal measured in double-sided p-type 3D strip detectors in a beam test as a function of bias voltage. Data are shown for one unirradiated detector and two detectors irradiated to 1.0×10^{15} and 2.0×10^{15} n_{eq}/cm^2, respectively.

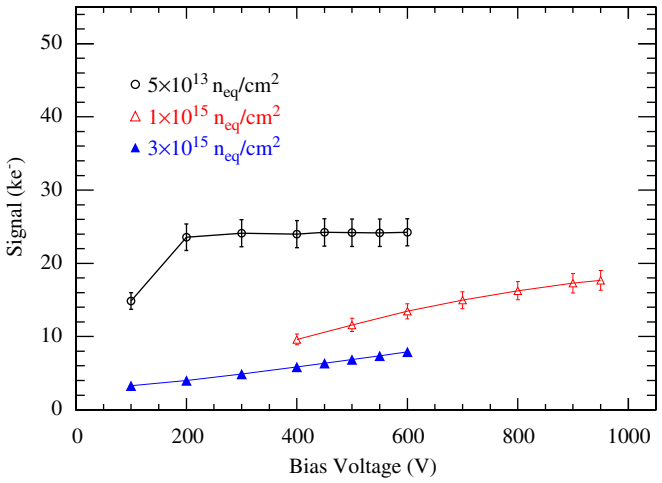

Fig. 5. Signal measured in planar p-type strip detectors in the same beam test as in Fig. 4. Signal values are given for three detectors irradiated to 5.0×10^{13}, 1.0×10^{15} and 3.0×10^{15} n_{eq}/cm^2, respectively.

have a higher impact ionisation coefficient than holes. We assume that the radiation-induced increase of the effective doping concentration, together with the higher electric field of 3D detectors compared to the planar design results in electric fields that are high enough to create a significant amount of charge multiplication already at comparatively low bias voltages around 200 V.

Similar effects have also been observed on heavily irradiated planar silicon strip detectors [20] and epitaxial silicon pad detectors [21]. However, for the planar and pad detectors much higher bias voltages were needed to see this effect. For a given external bias voltage, the design of the 3D detectors, in particular the short inter-column spacing with only 50 μm between n- and p-columns, results in much higher internal electric fields compared to other designs. This difference between the onset voltage of charge multiplication for planar and 3D detectors is clearly visible when comparing the signal measurement results for irradiated planar p-type detectors from the same test beam shown in Fig. 5 to the results from the 3D sensors in Fig. 4. Note the difference in voltage scale in these two figures. While the signal keeps on rising steadily with increasing bias, no clear evidence for charge multiplication is seen in the planar sensors up to the highest measured bias voltage of 1000 V. No charge multiplication effects were found in unirradiated planar or 3D detectors.

Comparisons of signal and leakage current measurements of the irradiated 3D detectors, which were both taken as a function of the bias voltage, show a strong correlation between the signal and the current [18]. Fig. 6 depicts signal and leakage current for the 3D detector irradiated to 1.0×10^{15} n_{eq}/cm^2. Both curves show very similar features with the hint of a plateau around 50–100 V and an increasing rise above around 150 V. This indicates that charges generated by traversing pions as well as the thermally generated charges that constitute the leakage current are multiplied by the same factor once the field is high enough for avalanche multiplication.

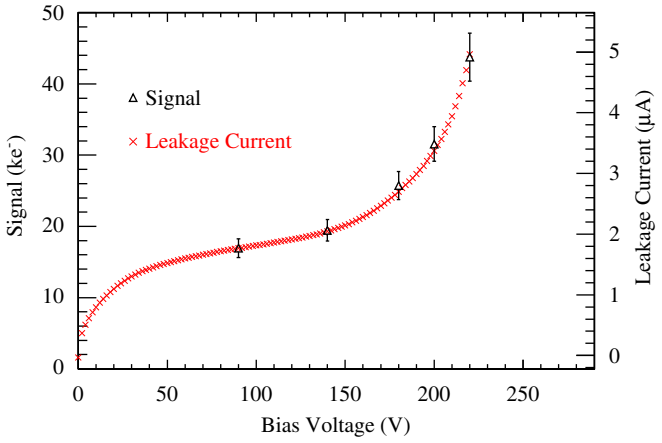

Fig. 6. Signal (black triangles) and leakage current (red crosses) measured in the 3D detector irradiated to 1.0×10^{15} n_{eq}/cm^2. The leakage current is measured at −20 °C. The current is the one from the strip area of the sensor, as the guard ring current was subtracted. (For interpretation of the references to color in this figure legend, the reader is referred to the web version of this article.)

6. Summary

Silicon tracking detectors have become the established standard detector technology to be used for the inner tracking layers of collider physics particle detectors. All four major LHC experiments successfully employ silicon vertex detectors. Experimental upgrades to cope with the luminosity increase by moving from the LHC to sLHC will also very likely centre around silicon-based detector systems. The extreme sLHC radiation levels pose a significant challenge that is met by the CERN RD50 Collaboration. In RD50, detector experts from a large number of experiments cooperate in several research lines in order to develop silicon detectors for sLHC applications.

Recent RD50 results from irradiations of different silicon materials such as FZ, MCz and EPI pad detectors show significant dependencies on the particle type used for irradiation, even if the irradiation is to the same equivalent fluence. For EPI detectors, the link between the microscopic defect responsible for the different effective doping concentrations after proton and neutron irradiations was found, explaining the different space charges seen in EPI detectors after proton and neutron irradiations. For n-type MCz detectors, a compensation of donors introduced by proton irradiation with acceptors generated by a subsequent neutron irradiation was reported.

Several studies show that p-type planar silicon detectors have sufficient radiation hardness to be operated up to fluences in the order of a few 10^{15} n_{eq}/cm^2, provided that a sufficiently high bias voltage exceeding can be supplied. 3D detectors would be able to

offer a comparable radiation hardness at significantly lower bias voltages. However, their design is more complex and the sensors are hence available only from a small number of suppliers and at a higher cost.

CCE measurements for irradiated planar, pad and 3D detectors have shown high signal levels that in some cases exceed the expected signal generated by a passing charged particle and can only be explained by a charge multiplication effect. Leakage current measurements demonstrate that the same mechanism also affects charges from thermal excitation. It appears likely that the underlying effect is impact ionisation and hence limited avalanche multiplication of charges drifting in the high electric field of the readout electrode.

A large number of miniature detectors with design variations expected to influence the charge multiplication effect have been produced and will be studied before and after irradiations as part of an ongoing RD50 project. Further longterm studies into the potential to exploit the charge multiplication effect for sLHC detectors are also ongoing.

Acknowledgements

The authors would like to thank the PS team for the PS proton irradiations carried out at CERN, the Ljubljana team for the TRIGA neutron irradiations and Karlsruhe Institute of Technology (KIT) for the cyclotron proton irradiations. The KIT irradiations were supported by the Initiative and Networking Fund of the Helmholtz Association, contract HA-101.

References

[1] G. Aad, et al., (ATLAS Collaboration), JINST3 7 (2008) P07007.
[2] R. Adolphi, et al., (CMS Collaboration), JINST3 8 (2008) P08004.
[3] RD50 Collaboration, RD50 Status Report 2008, CERN-LHCC-2010-012 and LHCC-SR-003.
[4] RD50 Collaboration 〈http://rd50.web.cern.ch/rd50〉.
[5] M. Huhtinen, Nucl. Instr. and Meth. A 491 (2002) 194.
[6] RD48 Collaboration 〈http://rd48.web.cern.ch/rd48〉.
[7] RD48 Collaboration, 3rd RD48 Status Report, CERN-LHCC-2000-009.
[8] I. Pintilie, G. Lindström, A. Junkes, E. Fretwurst, Nucl. Instr. and Meth. A 611 (2009) 52.
[9] I. Pintilie, M. Buda, E. Fretwurst, G. Lindström, J. Stahl, Nucl. Instr. and Meth. A 556 (1) (2006) 197.
[10] I. Pintilie, E. Fretwurst, G. Lindström, Appl. Phys. Lett. 92 (2) doi:10.1063/1.2832646.
[11] G. Kramberger, V. Cindro, I. Dolenc, I. Mandić, M. Mikuž, M. Zavrtanik, Nucl. Instr. and Meth. A 609 (2009) 142.
[12] A. Affolder, P. Allport, G. Casse, Nucl. Instr. and Meth. A 623 (2010) 177.
[13] A. Affolder, P. Allport, G. Casse, IEEE Trans. Nucl. Sci. NS-56 (2009) 765.
[14] S.I. Parker, C.J. Kenney, J. Segal, Nucl. Instr. and Meth. A 395 (1997) 328.
[15] A. Zoboli, M. Boscardin, L. Bosisio, G.-F. Dalla Betta, C. Piemonte, S. Ronchin, N. Zorzi, IEEE Trans. Nucl. Sci. NS-55 (2008) 2775.
[16] G. Pellegrini, M. Lozano, M. Ullan, R. Bates, C. Fleta, D. Pennicard, Nucl. Instr. and Meth. A 592 (2008) 38.
[17] T. Mäenpää, et al., Nucl. Instr. and Meth. A 593 (2008) 523.
[18] M. Köhler, et al., Beam test measurements with planar and 3D silicon strip detectors iradiated to sLHC fluences, IEEE Trans. Nucl. Sci., in press, doi:10.1109/TNS.2011.2126598.
[19] A. Zoboli, et al., IEEE Nuclear Science Symposium and Medical Imaging Conference (NSS - MIC'08), Conference Record, paper N34-4, Dresden (Germany), October 19–25, 2008.
[20] I. Mandić, V. Cindro, G. Kramberger, M. Mikuž, Nucl. Instr. and Meth. A 603 (2009) 263.
[21] J. Lange, J. Becker, D. Eckstein, E. Fretwurst, R. Klanner, G. Lindström, Nucl. Instr. and Meth. A 622 (2010) 49.